Simulations of Vacuum Arcs and Gas Discharges with Liquid Cathodes

Vladimir Kolobov, Dmitry Levko, Robert Arslanbekov

CFD Research Corporation
University of Alabama in Huntsville

Vladimir.Kolobov@cfdrc.com

8th International Workshop on Mechanisms of Vacuum Arcs
(MeVArc 2019)
15-19 September 2019
Orto Botanico – Padova, Italy

Background and Motivation

- **Simulations of vacuum arcs and gas discharges with liquid electrodes require coupling plasma physics with multi-phase flow science**
- **Specifics of gas breakdown and vacuum breakdown (volume processes vs surface processes)**
- **Computational challenges:**
  - **Different time scales for liquid dynamics and plasma dynamics (ms and ns, respectively)**
  - **Disparity of electron and ion time scales**
  - **Explosive Electron Emission: continuous phase transition (solid → liquid → gas → plasma)**
  - **Plasma expansion into vacuum or into a background gas vs ionization wave development**

Negative Corona on Liquid Water Cathode

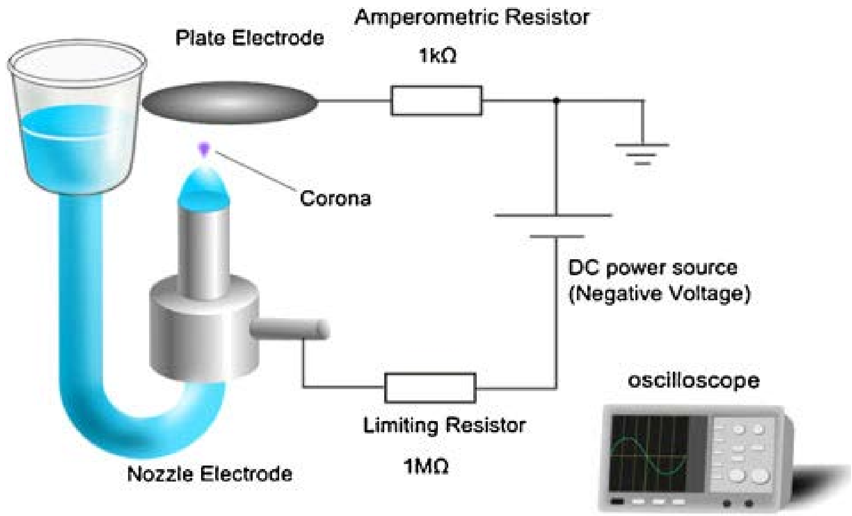

Experimental setup for corona discharge using Taylor cone

Atmospheric-pressure air
Cathode-anode gap is 5-20 mm

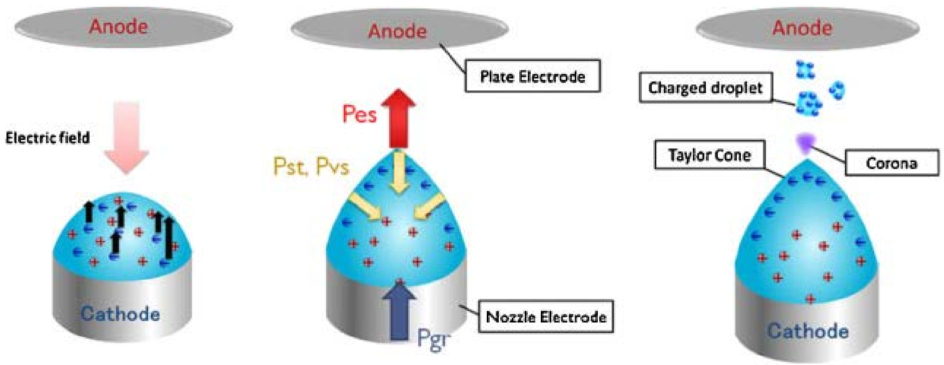

Principle of Taylor cone formation. (a) Initial state, (b) Taylor cone formation, and (c) Corona discharge at the tip of Taylor cone

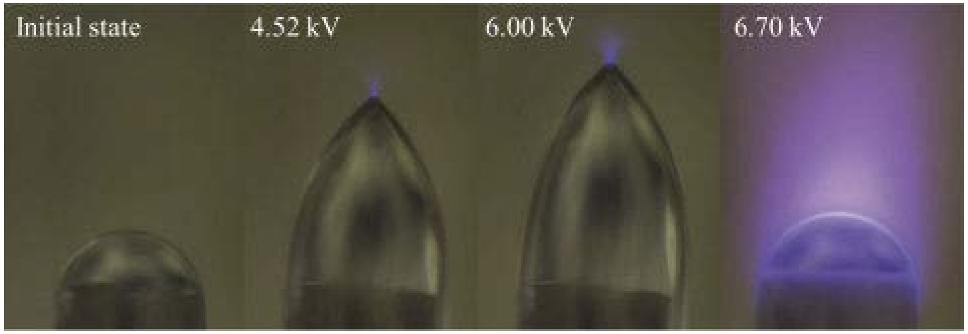

Corona discharge using Taylor cone and shape of the liquid surface

N. Shirai, R. Sekine, S. Uchida, and F. Tochikubo, Atmospheric negative corona discharge using Taylor cone as a liquid cathode, JJAP **53,** 026001 (2014)

Computational Model for Liquid Dynamics

Navier-Stokes equation for two-phase flows:

$$\nabla \cdot \boldsymbol{u} = 0$$

$$\rho \frac{\partial \boldsymbol{u}}{\partial t} + \rho(\boldsymbol{u} \cdot \nabla)\boldsymbol{u} = \nabla \cdot \left[-p\boldsymbol{I} + \mu\left(\nabla \boldsymbol{u} + (\nabla \boldsymbol{u})^T\right)\right] + \frac{p}{l}\boldsymbol{n}$$

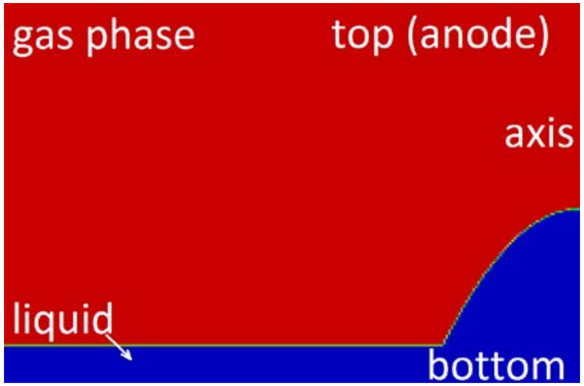

Gas-liquid interface tracked using Volume- of-Fluid method, http://basilisk.fr

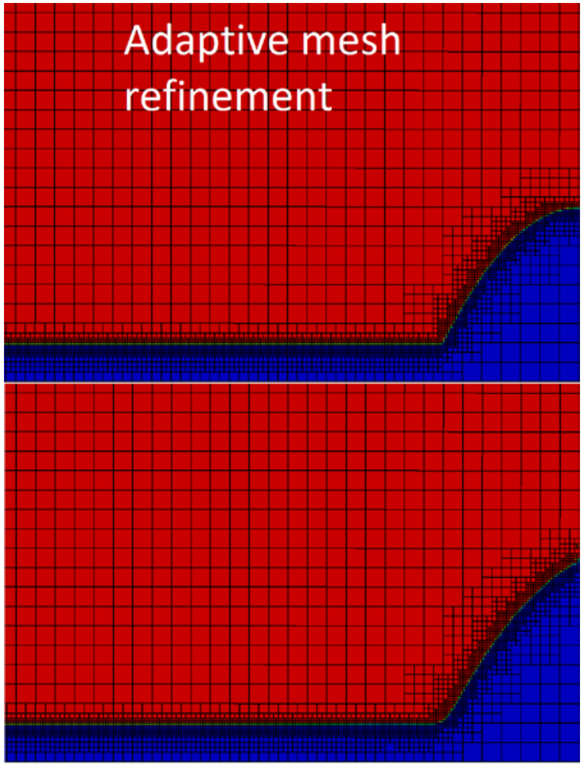

Two competitive forces at interface: surface tension and electrostatic

Laplace equation for electrostatic potential

$$\Delta\varphi = 0$$

$$\varphi_{top} = 0, \;\; \varphi_{bottom} = \varphi_0$$

Time scale is milliseconds → $\Delta t \sim 10^{-7} – 10^{-6}$ s

Dynamics of Taylor Cone Formation in Electric Field

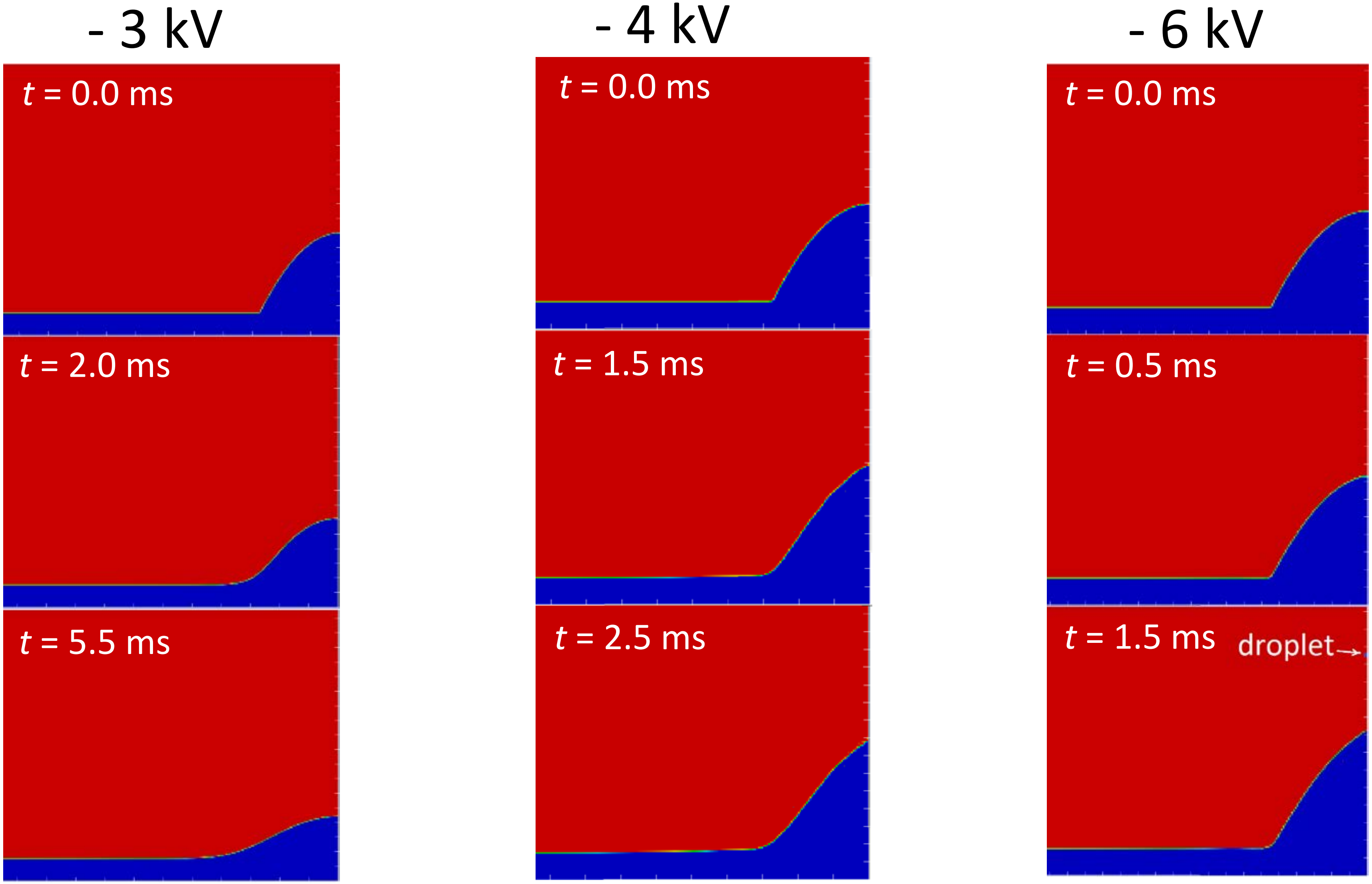

- Interplay between surface tension and electrostatic forces leads to Taylor cone formation
- The cone development terminates with droplet ejection from the tip (electrospray)
- Voltage influences the cone shape and height, and the droplet ejection rate

Gas Breakdown: Electron Kinetics

$$\frac{\partial f_e}{\partial t} + v\frac{\partial f_e}{\partial x} - \frac{eE-F(v)}{m_e}\frac{\partial f_e}{\partial v} = S_{ion}(v)$$

$$S_{ion}(v) = S(v)\int_{-\infty}^{+\infty} n_g \sigma_{ion}(v') f_e(x,v',t)\,dv'$$

$$n_e = \int_{-\infty}^{+\infty} f_e\,dv$$

$$F(\varepsilon_e) = \frac{e^4 Z n_g}{8\pi\varepsilon_0^2\varepsilon_e}\cdot \ln\left(\frac{\varepsilon_e}{I}\right), \text{where } \varepsilon_e = \frac{m_e v^2}{2}$$

$$\frac{dn_i}{dt} = S_{ion} \qquad \frac{d^2\varphi}{dx^2} = \frac{e}{\varepsilon_0}(n_e - n_i)$$

400 Torr, initial plasma density 2×10^{11} m^{-3}, gap d = 6 mm, *dU/dt* = 8.4×10^{10} V/s, σ_{ion} = 2×10^{-20} m^{-2}

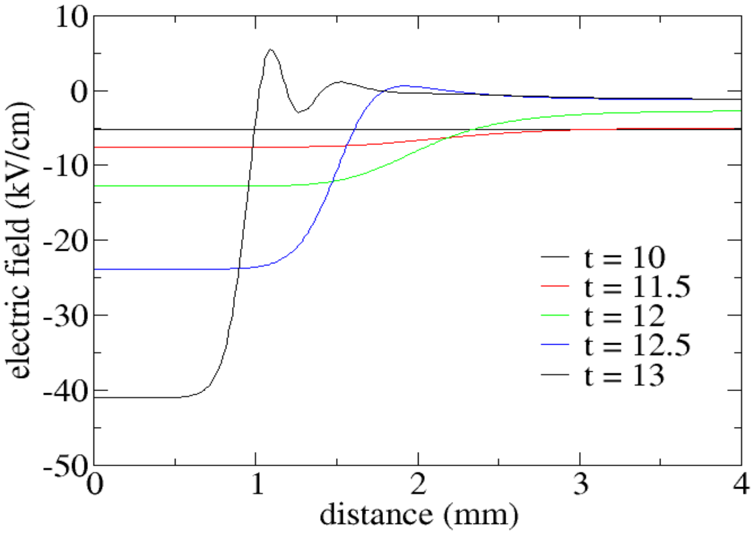

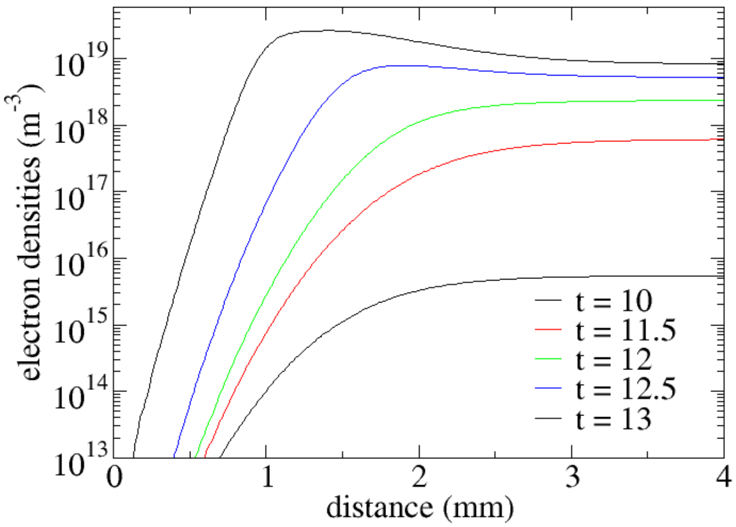

Kolobov et al, Boltzmann-Fokker-Planck Kinetic Solver with Adaptive Mesh in Phase Space, AIP Conf. Proc. 2132, 060011 (2019); https://doi.org/10.1063/1.5119551

Fluid Model: Gas Breakdown and Plasma Formation

Drift-diffusion approximation for both electrons and ions:

$$\frac{\partial n_k}{\partial t} + \nabla \cdot \Gamma_k = S_k$$

$$\Gamma_k = -\mu_k n_k \nabla\varphi - D_k \nabla n_k$$

Electron energy balance:

$$\frac{\partial \varepsilon_e}{\partial t} + \nabla \cdot \Gamma_\varepsilon = S_\varepsilon$$

Poisson equation for the electrostatic potential:

$$\Delta\varphi = \frac{q_e}{\varepsilon_0}(n_e - n_i)$$

Dynamics of Gas Breakdown

Mesh is adapted on (n_e-n_i)

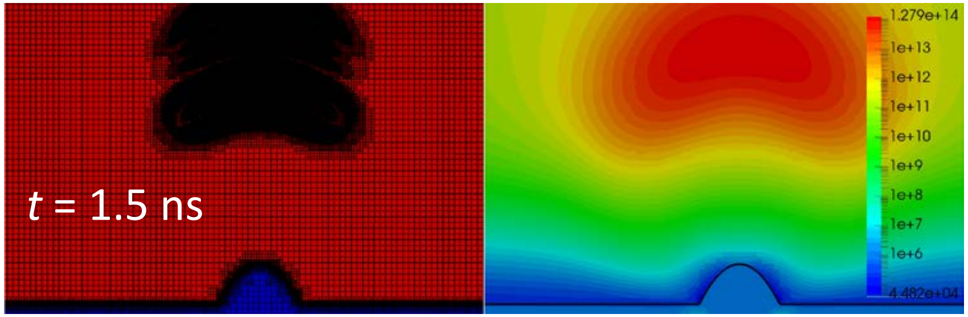

Mesh is adapted on field

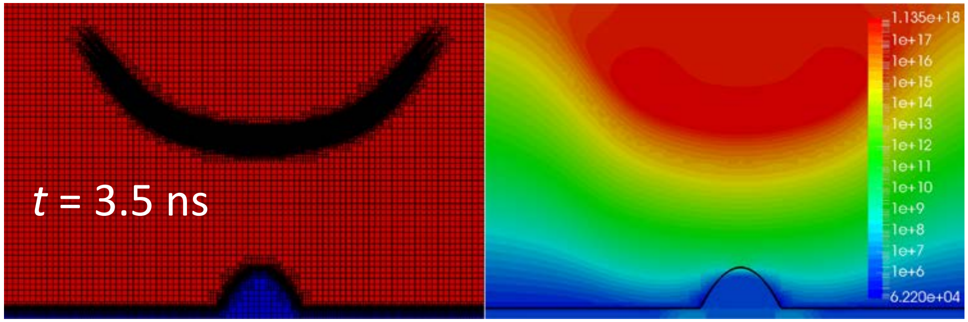

Quasi-neutral plasma near the anode

Time scale is nanoseconds → $\Delta t \sim 10^{-14} - 10^{-12}$ s

Paschen Curves for Pulsed Gas Breakdown

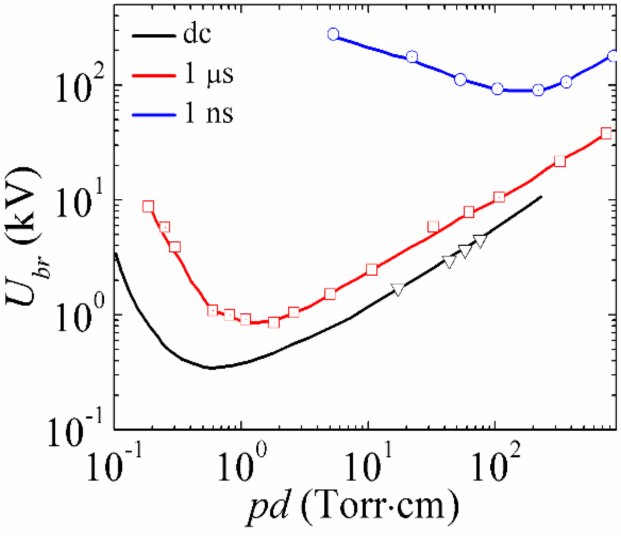

- **Voltage rise time *τ* affects the Paschen curves for planar gaps.**
- **Both kinetic and fluid models predict the experimentally observed shift of the curves toward higher voltages and the shift of Paschen minima toward higher *pd* with decreasing *τ*.**
- **On the right branch, the agreement between both models is obtained for all *τ*.**
- **The fluid model could not describe the left branch of the Paschen curves.**

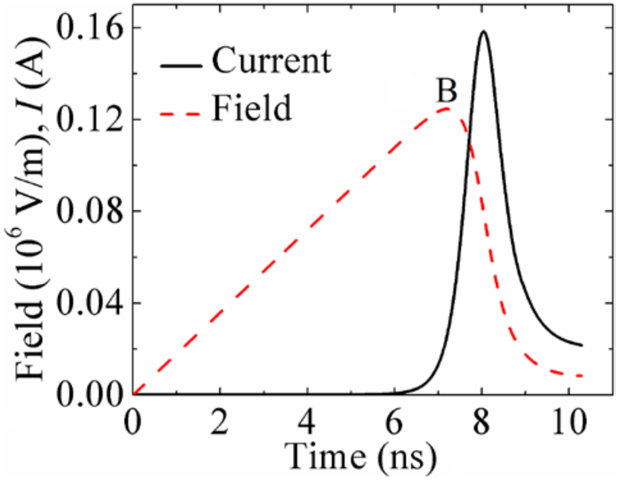

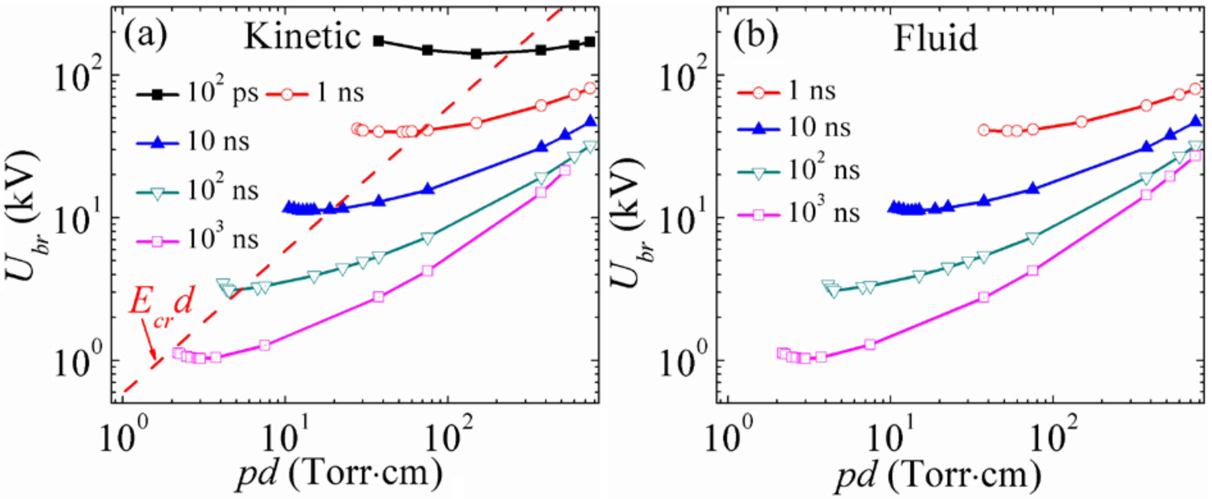

Levko et al, Modified Paschen curves for pulsed breakdown, Phys. Plasmas 26, 064502 (2019)

Dynamics of Corona Discharge Development

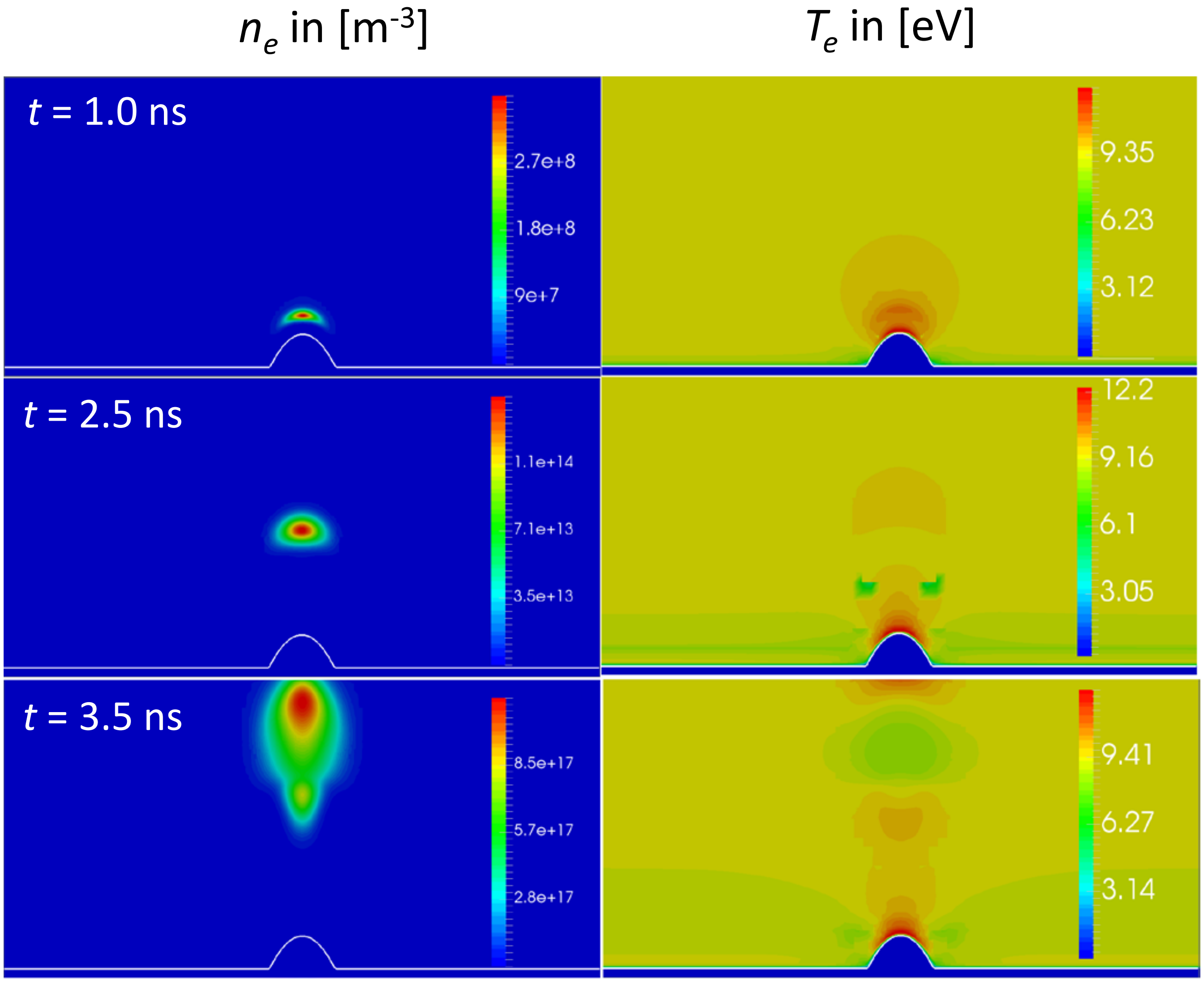

n_e in [m^{-3}]

T_e in [eV]

Negative corona discharge is ignited at low voltages; ionization wave propagates toward the anode

Plasma density does not exceed 10^{15} m^{-3}; Electric field remains undistorted; Highest T_e is obtained at the cone tip

Primary avalanche leaves behind uncompensated positive space charge; ions propagate to the cathode on much longer time scale

Dynamics of Glow Discharge Development

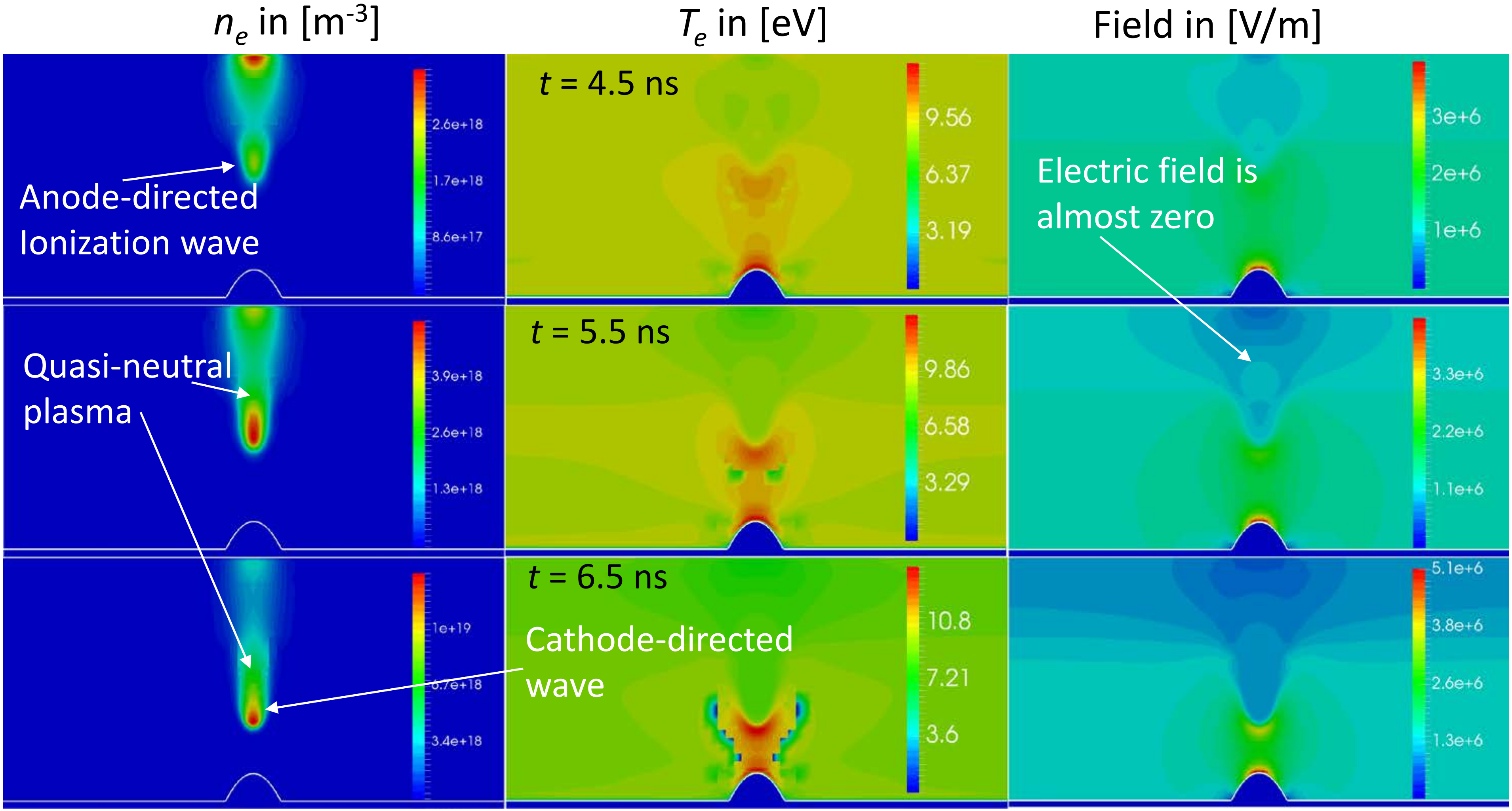

t = 4.5 ns

t = 5.5 ns

t = 6.5 ns

Anode-directed Ionization wave

Electric field is almost zero

Quasi-neutral plasma

Cathode-directed wave

The anode-directed ionization wave stops and follows the fast-axial wave propagating towards the cathode: the cathode sheath is formed. Further development of the discharge occurs at the (slow) ion time scale.

Discharge formation between cone tip and droplet

The cone growth stops once droplets are ejected from the tip; they shield the electric field

Electric field sufficient for gas breakdown is obtained between the cone tip and the droplet

Plasma density in the vicinity of the cathode is ~10^{21} m^{-3} and keeps growing; sheath thickness is <0.1 µm

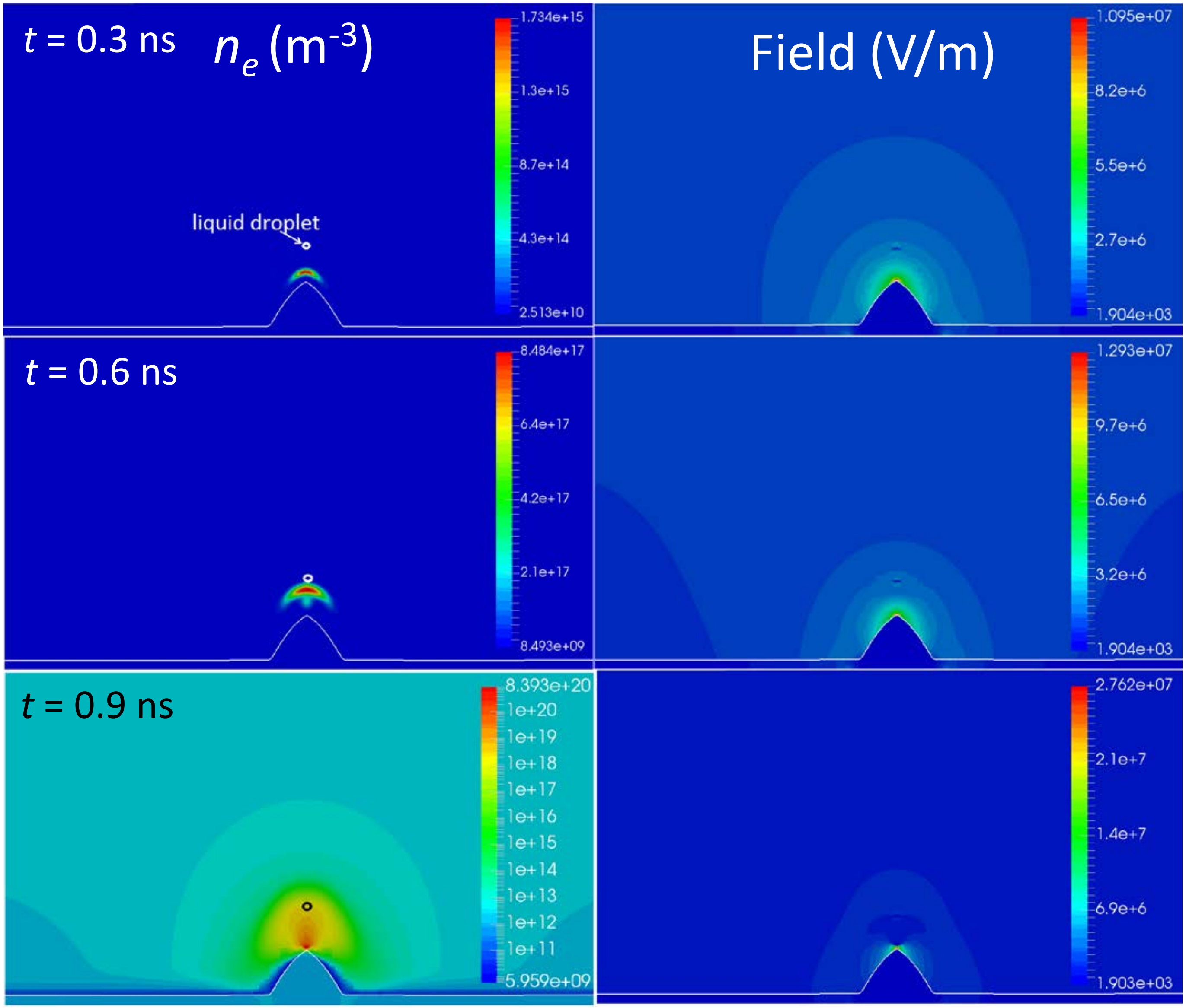

Explosive Electron Emission in Vacuum Arcs

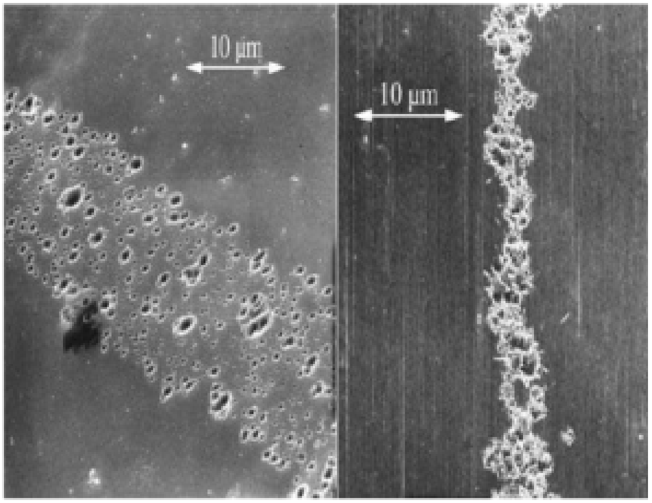

Arc traces on cathode left by vacuum arcs

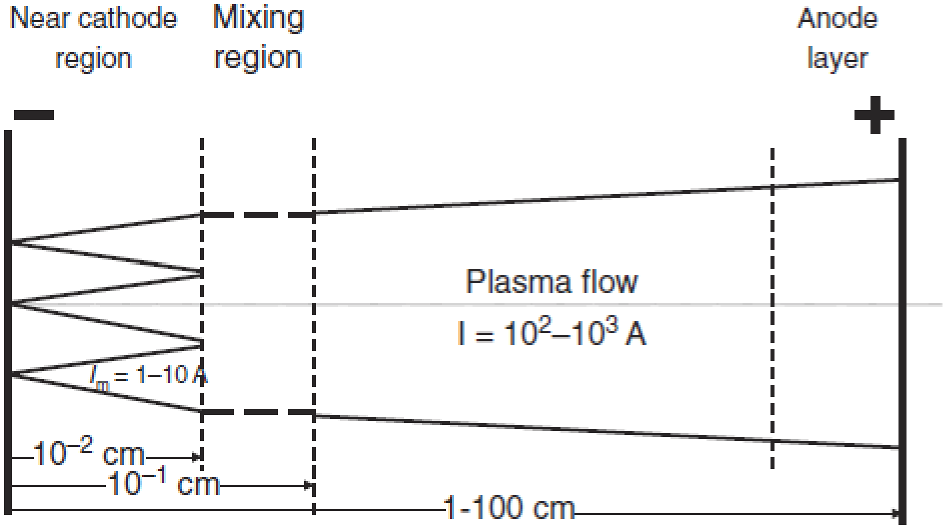

Schematic diagram of vacuum arc discharge

- A distinctive feature of electric discharges in a vacuum is rapid phase transitions of the cathode material from a solid state to liquid, gaseous, and plasma states
- The plasma state changes from a dense non-ideal to a moderately rarefied, and to a collisionless.
- The cathode material is emitted from micro-explosions (ectons) and progressively accelerated to velocities of about 10^6 cm/s, the particle density decreases from 10^{23} to 10^{10} cm^{-3}

Vacuum Discharge Ignition from Liquid-Metal Cathodes

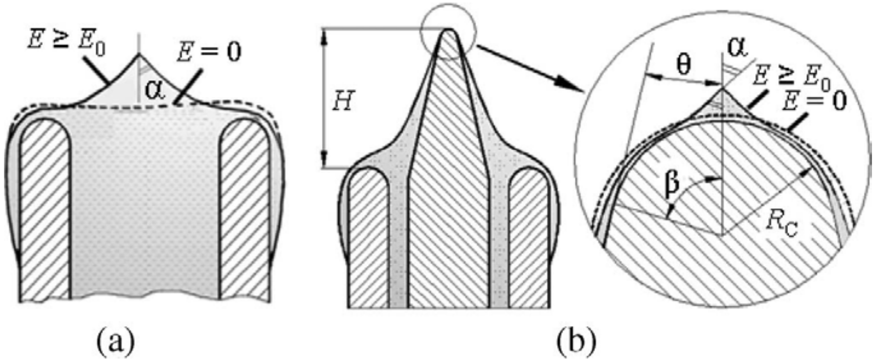

Types of liquid metal cathodes

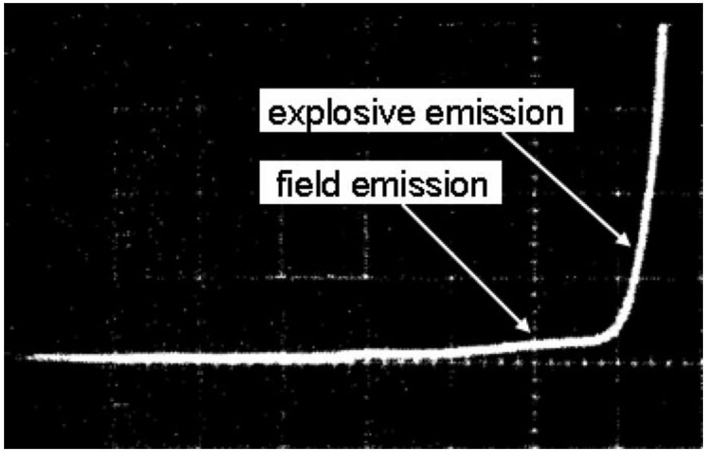

Electron emission current oscillogram
L. W. Swanson and G. A. Schwind, J. Appl. Phys. 49, 5655 (1978)

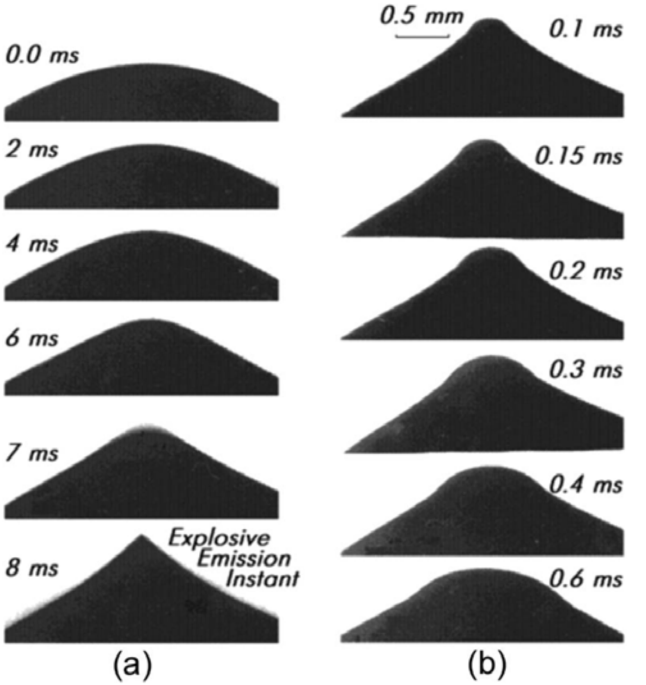

Shadow photographs showing (a) growth and (b) decay of a protrusion on the liquid metal cathode with diameter 4 mm

InGa is liquid at room temperature

D.I. Proskurovsky, Explosive Electron Emission From Liquid-Metal Cathodes, IEEE TPS **37,** 1348 (2009)

Taylor cone formation on Liquid Metal Cathode

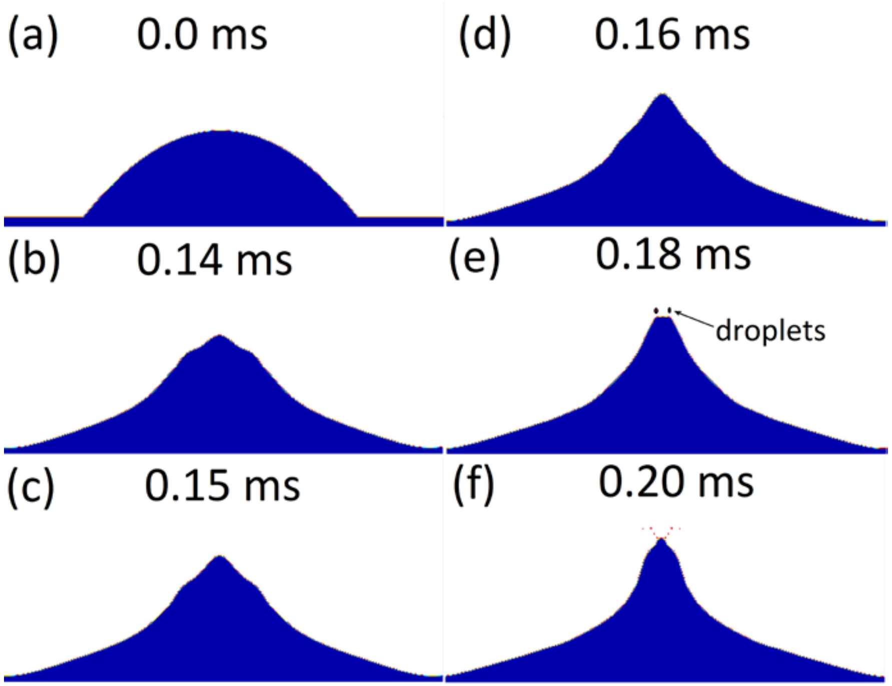

Conditions:

InGa liquid cathode
Cathode potential -40 kV
Cathode-anode gap is 2 mm

- Electric field at the cathode tip increases with time
- Unstable Taylor cone is formed during 0.2 ms
- Liquid droplets are ejected from the cone tip
- Droplet ejection precedes the field emission onset

Electric field distribution (10^8 V/m)

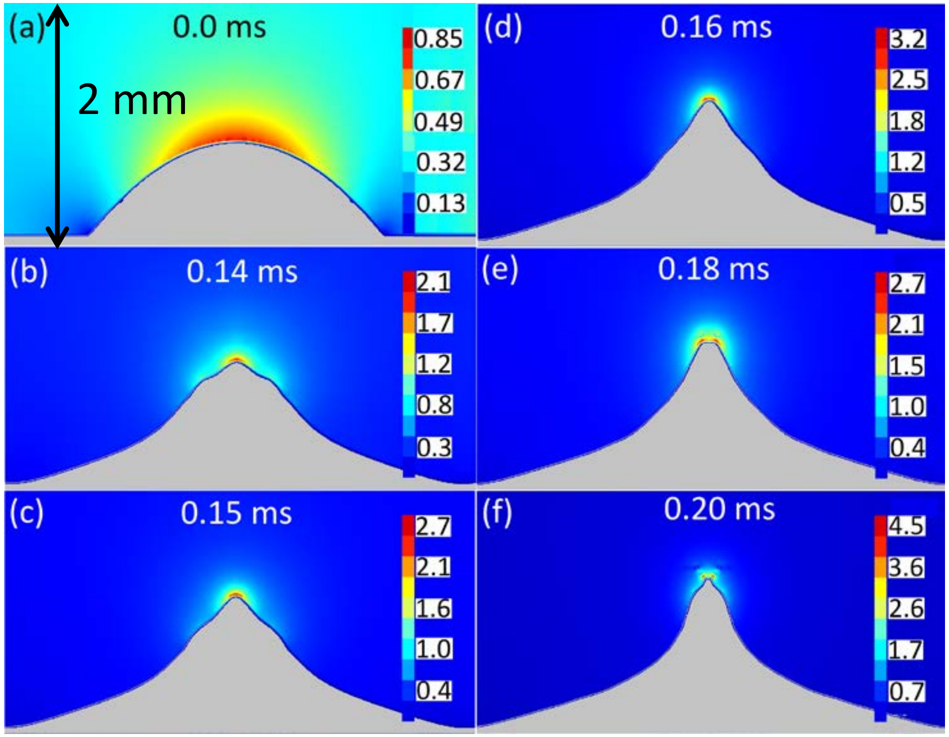

Liquid Metal Protrusion Heating

Axisymmetric model of micro-protrusion heating:

$$\rho C_p \frac{\partial T(\boldsymbol{r},t)}{\partial t} = \nabla(\lambda(T)\nabla T(\boldsymbol{r},t)) + F(\boldsymbol{r},t)$$

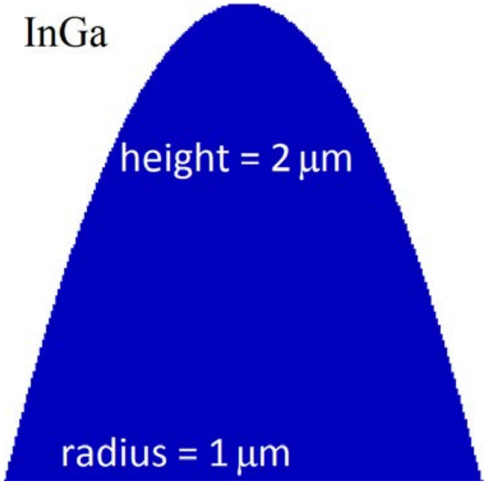

Heating is due to electric current and Thomson effect:

$$F(\boldsymbol{r},t) = \boldsymbol{j}(\boldsymbol{r},t)\boldsymbol{E}(\boldsymbol{r},t) + g(T)(\boldsymbol{j}(\boldsymbol{r},t)\nabla T(\boldsymbol{r},t))$$

Solve the Poisson's equation to define the current density:

$$\nabla[\sigma(T)\nabla\varphi(\boldsymbol{r},t)] = 0 \quad \rightarrow \boldsymbol{j}(\boldsymbol{r},t) = \sigma(T)\nabla\varphi(\boldsymbol{r},t)$$

Boundary conditions:

$$\lambda(T)\frac{\partial T(\boldsymbol{r},t)}{\partial \boldsymbol{n}} = \frac{j_{FE}\left(E_{surf},T_{surf}\right)}{e}\Delta E\left(E_{surf},T_{surf}\right) - \sigma_{SB}T_{surf}^4$$

$$\sigma(T)\frac{\partial\varphi(\boldsymbol{r},t)}{\partial \boldsymbol{n}} = j_{FE}\left(E_{surf},T_{surf}\right)$$

$g(T)$ is the Thomson constant, $\sigma(T)$ is the conductivity, ΔE energy carried out by emitted electrons; takes into account the Nottingham effect, σ_{SB} is the Stefan-Boltzmann constant, and $j_{FE}\left(E_{surf},T_{surf}\right)$ is the known function of the emitter shape

from Glazanov, Baskin and Fursey, Journal of Technical Physics **59,** 60 (1989)

Liquid Metal Protrusion Heating

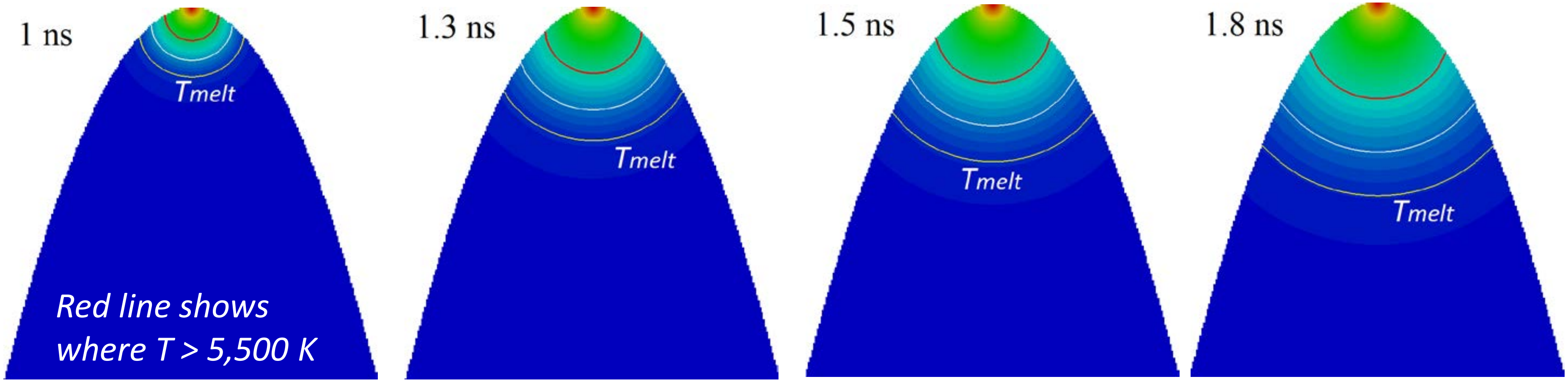

Red line shows where T > 5,500 K

Temperature in the protrusion bulk (1.7 µm from the bottom)

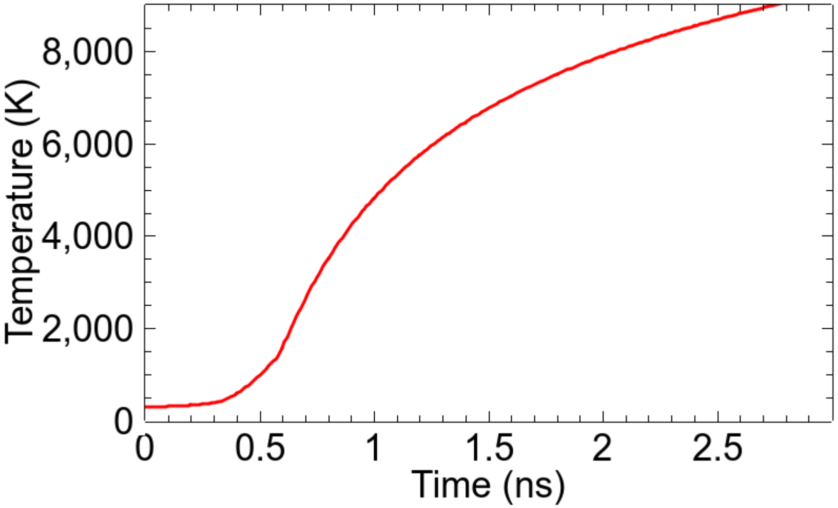

- Thermal instability develops only when the current density at the tip exceed 10^8 A/cm^2 in agreement with the Mesyats' theory
- Then, the micro-protrusion temperature at the tip starts exceeding the boiling temperature on the ns time scale
- This clearly indicates that the field-to-explosive electron emission occurs after 1 ns
- Now we know the metal mass which experiences phase transition from solid to non-ideal plasma: can use it for plasma expansion modeling;

Plasma Expansion: Gas-Dynamic LTE Model

LTE model is widely used for pulsed laser ablation (Saha equation)

Adaptive Computation Domain

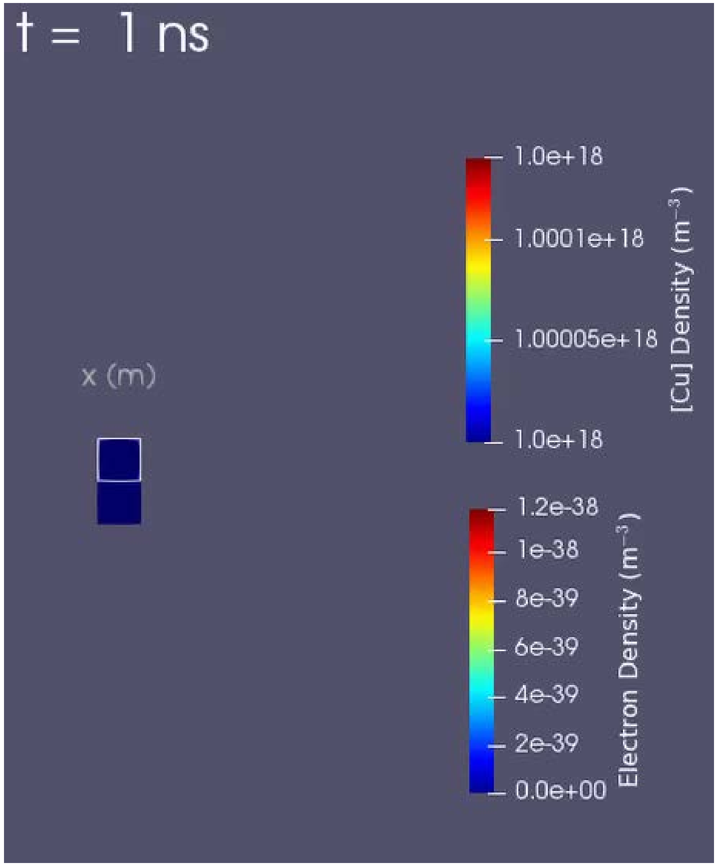

- **Implemented 2D planar and axisymmetric solvers with ACD**
- **Generic EOS to describe continuous phase transition**

Dynamically Adaptive Cartesian Mesh

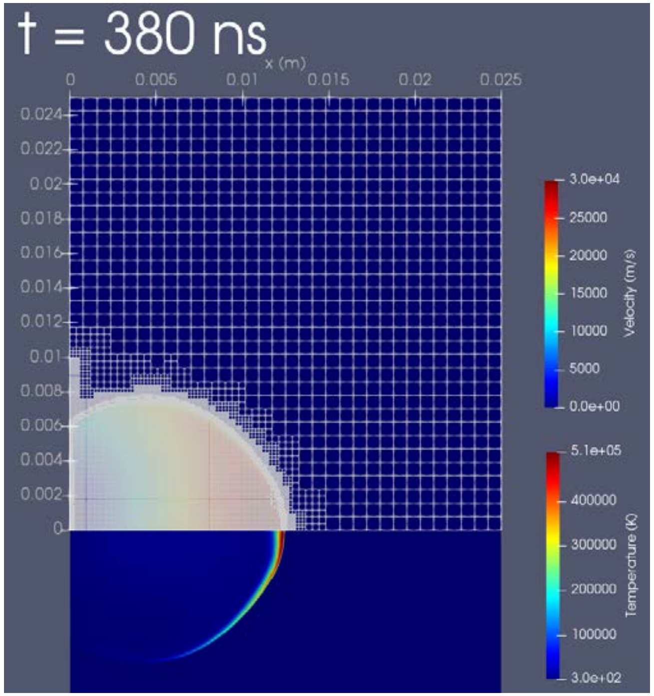

Fluid Model for Plasma Expansion into Vacuum

Collisionless, cold ions, Boltzmann-electron model:

$$\frac{\partial n_i}{\partial t} + \nabla \cdot (n_i \vec{u}_i) = 0,$$

$$m_i \frac{\partial \vec{u}_i}{\partial t} + m_i (\vec{u}_i \cdot \nabla) \vec{u}_i = -e \nabla \varphi,$$

$$\nabla^2 \varphi = \frac{e}{\epsilon_0} (n_e - n_i)$$

$$n_e = n_0 \exp\left(\frac{e\varphi}{k_B T_e}\right)$$

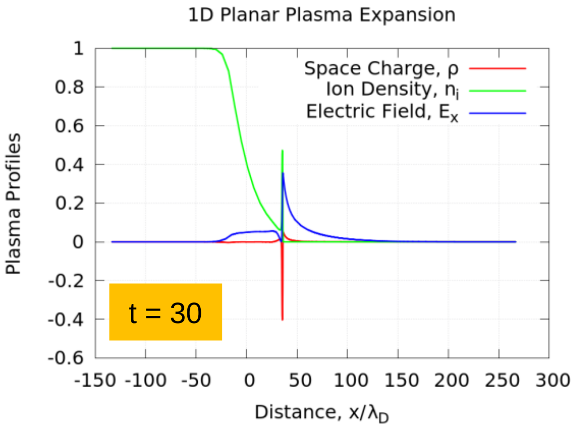

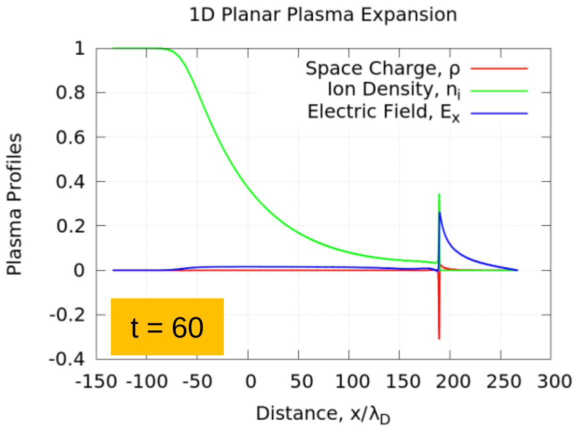

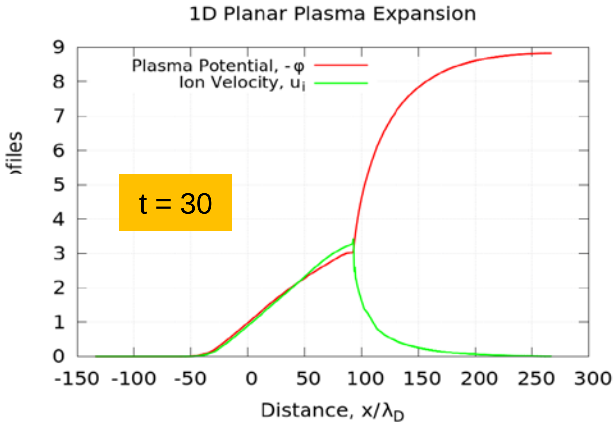

Very sharp ion density peaks predicted (peak widths a few λ_D)

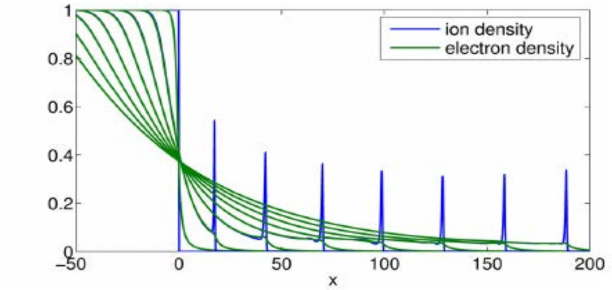

J. E. Allen and M. Perego, On the ion front of a plasma expanding into a vacuum, Physics of Plasmas 21, 034504 (2014);

- Good agreement with other 1D computations using both Eulerian and Lagrangian approaches. Both spatial and temporal profiles are well reproduced
- The code can be used to study collisionless plasma expansion dynamics in multi-dimensions

Plasma Expansion: Influence of External Field

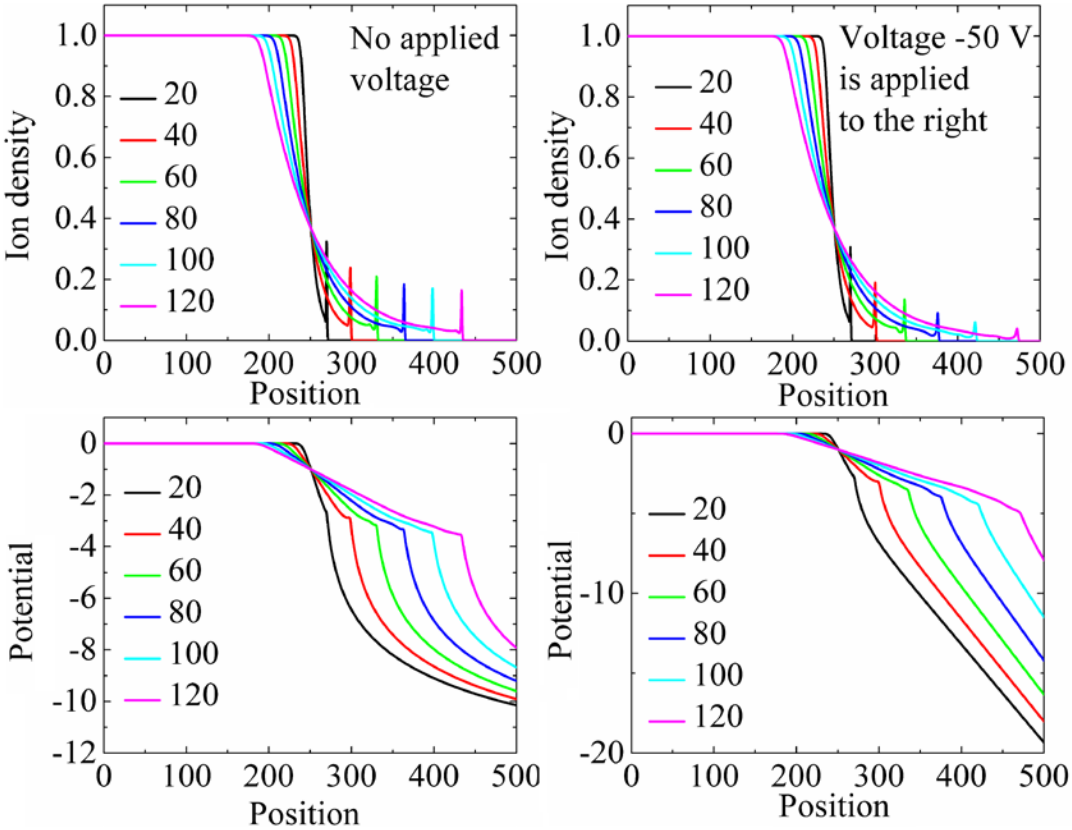

Ion front in both cases

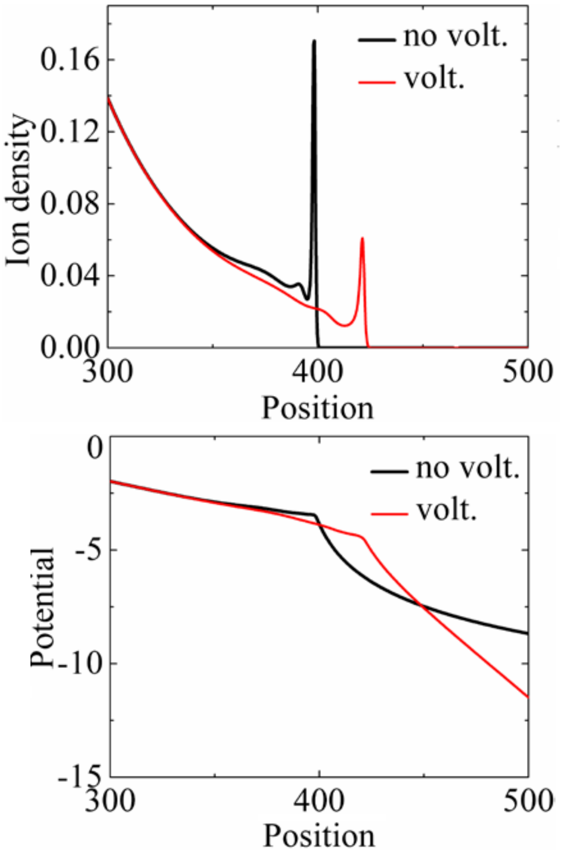

Gap $1000\lambda_D$

Voltage $\sim 50T_e$

- **Applied voltage starts influencing the plasma front propagation only when it is far from the “core” dense plasma: the plasma density decreases → Debye length decreases → external electric field starts penetrating the plasma**
- **Front velocity increases with time because the electric field between the front and the right boundary increases with time**

Two Types of Positive Ions

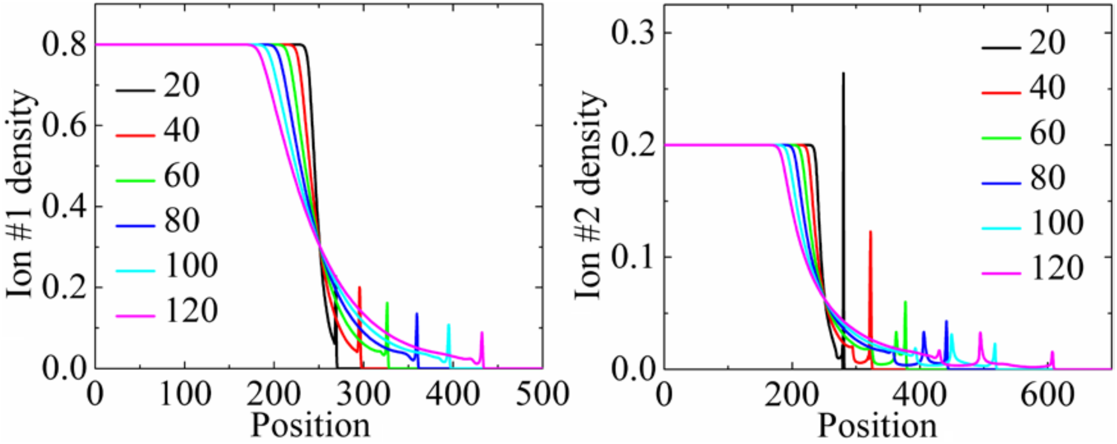

$$\frac{Z_1}{Z_2} = \frac{1}{2}$$

$$\frac{n_1}{n_2} = \frac{8}{2}$$

Comparison with 1 ion plasma expansion

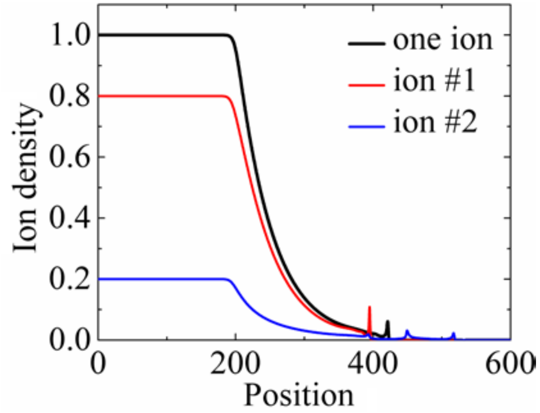

- Ions with larger charge propagate faster
- Density of Ion #2 has multipeak structure: the 1st peak coincides with the position of the Ion #1 peak, and the 3rd peak is the ion front
- All the peaks are formed at different stages: the 3rd peak is formed at the earliest stage of the front formation
- Velocity of the Ion #1 only slightly depends on the applied voltage
- Velocity of the Ion #2 increases with time
- Ion #1 moves slower than in the case of one ion species plasma

Conclusions

- We have developed computational models for multi-phase plasmas with adaptive Cartesian mesh
- Simulated dynamics of Taylor cone formation on liquid cathodes using Volume-of-Fluid model
- Illustrated development of Corona and Glow Discharges with liquid cathodes
- Plasma expansion into vacuum has been simulated with fluid models
- Adaptive Computation Domain methodology has been introduced
- The differences between gas breakdown and vacuum breakdown have been identified and illustrated

Outlook

- Combine fluid and kinetic models for expanding plasma
- Simulate dynamics of vacuum breakdown and clarify effects of anode processes
- Quantify effects of background gas pressure on electron emission and volume ionization processes during breakdown and plasma formation
- Identify mechanisms of nano-particle production during adiabatic expansion of dense plasma into vacuum and background gas
- Identify similarities and differences between pulsed laser ablation (from fs to ns scales) and dynamics of spark and arc discharges

Acknowledgements

- DoE SBIR Phase II Contract DE- DE-SC0015746 “Simulations of Explosive Electron Emission in Cathodic Arcs”

- NSF EPSCoR project OIA-1655280 “Connecting the Plasma Universe to Plasma Technology in AL: The Science and Technology of Low-Temperature Plasma”